Chinese Chemical Letters 35 (2024) 109183

Contents lists available at ScienceDirect

Chinese Chemical Letters

journal homepage: www.elsevier.com/locate/cclet

Cucurbit[7]uril confined phenothiazine bridged bis(bromophenyl pyridine) activated NIR luminescence for lysosome imaging

Hui-Juan Wang[a,b,1], Wen-Wen Xing[a,1], Zhen-Hai Yu[a], Yong-Xue Li[a], Heng-Yi Zhang[a], Qilin Yu[c], Hongjie Zhu[b], Yao-Yao Wang[b], Yu Liu[a,*]

[a] College of Chemistry, State Key Laboratory of Elemento-Organic Chemistry, Nankai University, Tianjin 300071, China
[b] Shandong Provincial Key Laboratory of Chemical Energy Storage and Novel Cell Technology, School of Chemistry and Chemical Engineering, Liaocheng University, Liaocheng 252000, China
[c] Key Laboratory of Molecular Microbiology and Technology, College of Life Sciences, Nankai University, Tianjin 300071, China

ARTICLE INFO

Article history:
Received 27 July 2023
Revised 27 September 2023
Accepted 7 October 2023
Available online 10 October 2023

Keywords:
Phenothiazine
Supramolecular assembly
Macrocycle confined
Probe
HClO/ClO⁻

ABSTRACT

Macrocycle confinement induced guest near-infrared (NIR) luminescence was research hotspot currently. Here in, we reported a cucurbit[7]uril (CB[7]) confined 3,7-bis((*E*)-2-(pyridin-4-yl)vinyl)-10-*H*-phenothiazine bridged bis(4-(4-bromophenyl)pyridine) (**G**), which not only boosted its NIR luminescence but also realized detection of HClO/ClO⁻ in living cells and lysosome imaging. Fluorescence spectroscopy experiments were performed to calculate the detection ability of probe **G** to HClO/ClO⁻ up to 147 nmol/L. As compared with **G**, supramolecular probe **G**⊂CB[7] formed after encapsulated by CB[7], the detection ability towards HClO/ClO⁻ was improved to 24 nmol/L which was ascribe to the macrocycle CB[7] confinement increasing the fluorescence intensity to 103 folds. Accompanying the excitation wavelength changing, the fluorescence red-shifted to 820 nm when excited by 570 nm light, which was used to NIR lysosome imaging. Meanwhile, the supramolecular assembly **G**⊂CB[7] was also successfully used to highly sense to exogenous HClO/ClO⁻ in RAW 264.7 cells and live animal.

Supramolecular macrocycle confinement not only induced guest phosphorescence/fluorescence enhancement, but also generate delayed fluorescence through cascade assembly, which was the hot research at present [1–6]. During the research of macrocycle confinement, macrocycle cucurbit[*n*]urils (CB[*n*]s) with hydrophobic cavity formed by acid catalyzed condensation of glycoluril and formaldehyde can encapsulated guests to avoid nonradiative transition and boosted phosphorescence [7]. CB[*n*]s confined phosphorescence materials were widely applied to biological imaging [8,9], luminescent materials [10], anti-counterfeiting [11,12] and so on. Liu *et al.* reported a series of CB[8] confinement induced and enhanced phosphorescence materials based on 4-(4-bromophenyl)pyridine derivatives. For example, 4-(4-bromophenyl)pyridine modified hyaluronic acid (HA) encapsulated by CB[8] formed biaxial pseudorotaxane polymer with phosphorescence, which was used to mitochondria-targeted tumor cell phosphorescence imaging [13]. When photo-responsive group anthracene was modified to 4-(4-bromophenyl)pyridine and encapsulated by CB[8], a linear polymer with photo-switchable fluorescence/phosphorescence was obtained, which was successfully applied to nuclei and lysosomes fluorescence/phosphorescence imaging, respectively [14]. On the other hand, CB[6] confined phenylmethylpyridinium also achieved several solid-state supramolecular ultralong lifetimes and ultrahigh quantum yields phosphorescence materials and used to anti-counterfeiting [15,16]. Recently, we reported a γ-cyclodextrin confined 2-triphenylene boronic acid modified poly(vinyl alcohol) and constructed a system with full color afterglow lasted more than 50 s through phosphorescence energy transfer, which was used to noctilucent lighting and anti-counterfeting ink [17]. Tian and Ma *et al.* reported a multistimulus-responsive small molecule crystal bis(4-alkoxyphenyl)ethane-1,2-dione which can be tuned by thermal annealing and grinding to achieve blue and yellow phosphorescence [18]. Tang, Li and Yang *et al.* reported a long-lived phosphorescence material based on β-cyclodextrin confined *p*-biphenylboronic acid and realized tuning the colors of afterglow through phosphorescence energy transfer [19]. Although many macrocycle confined optical materials were reported, it is still no reports about the macrocycle confined guest for detection of conjugate acid-base pair HClO/ClO⁻, to the best of our knowledge.

* Corresponding author.
E-mail address: yuliu@nankai.edu.cn (Y. Liu).
[1] These authors contributed equally to this work.

https://doi.org/10.1016/j.cclet.2023.109183
1001-8417/

Conjugate acid-base pair HClO/ClO^- is a common type of reactive oxygen species (ROS), which was formed through the heme enzyme myeloperoxidase (MPO) catalyzed reaction of hydrogen peroxide and chloride *in vivo* and played a crucial role in numerous cellular functions [20–22]. The excess production of HClO/ClO^- is closely related to a variety of diseases, such as rheumatoid arthritis (RA), osteoarthritis, neurological diseases, cardiovascular diseases even cancer [23,24]. Among them, the incidence rate of RA is very high, and the destruction rate of bone and joint reached to 50% two years before the onset [25]. Early diagnosis and treatment of RA can effectively prevent joint erosion [26]. Considering the highly reactive and short-lived nature of HClO as the biomarker of RA in organism [27], it is urgent to explore fast responsive and highly sensitive HClO probes to real-time monitoring the action of cellular HClO. Currently, many fluorescent probes based on fluorochromes modified by HClO responsive groups were reported, such as chalcogenide, hydrazine, hydrazone, oximes, double bond and schiff base [20]. Liu and Li *et al.* designed a quinolone derivatives with two-photon fluorescence response to HClO which was successfully used to monitoring HClO *in situ* in the wounded tissues of mice [28]. Li *et al.* reported a resorufin derivative with amine which can be oxidative cleavage by HClO and realized visualization of HClO in cells, zebrafish and mouse [29]. The phenothiazine core was a well-defined electron donor whose absorbance and fluorescence are easily to change by the protonation or oxidation [30]. Recently, Xiong *et al.* reported a pH sensitive and HClO actived fluorescent probe based on 3,7-bis((*E*)-2-(pyridin-4-yl)vinyl)-10-*H*-phenothiazineand used to detect RA [31]. Huang, Yin and Wang *et al.* reported two fluorescent probes with remarkable selectivity toward HClO through linked phenothiazine to diaminomaleonitrile by imine bonds and were successfully used to detect HClO in zebrafish [32]. But most of them showed low water solubility, complex synthesis process and high biological toxicity. Supramolecular chemistry provides an easy and feasible method to avoid these troubles. Here, we synthesized 3,7-bis((*E*)-2-(pyridin-4-yl)vinyl)-10-*H*-phenothiazine bridged bis(4-(4-bromophenyl)pyridine) (**G**) which showed high sensitivity to oxidizing agent even to air. The encapsulation by CB[7] can increase the stability of **G** in air and showed HClO/ClO^- activable fluorescence. Finally, the supramolecular probe **G**⊂CB[7] was successfully used to detect HClO/ClO^- *in vivo* and *in vitro* (Scheme 1).

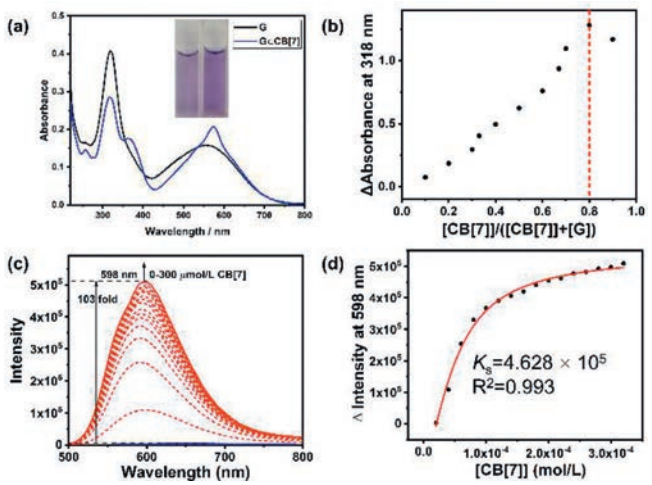

Fig. 1. (a) UV-vis absorbance spectra of **G** and **G**⊂CB[7] ([**G**] = 4×10^{-5} mol/L, [CB[7]] = 1.6×10^{-4} mol/L). (b) Job plot of **G** and CB[7] according to the absorbance at 318 nm ([CB[7]]+[**G**] = 2×10^{-4} mol/L). (c) Fluorescence spectra of **G** ([**G**] = 5×10^{-5} mol/L) with the addition of CB[7] (0-300 μmol/L, λ_{ex} = 470 nm). (d) Nonlinear least squares fit of the fluorescence changes at 598 nm of **G** upon addition of CB[7]. Solvent: water.

Compound **G** was obtained through the conjugation of 4-(4-bromophenyl)pyridine (PY) and 3,7-bis((*E*)-2-(pyridin-4-yl)vinyl)-10-*H*-phenothazine (Scheme S1 in Supporting information) and its corresponding characterizations were shown in Figs. S1–S3 (Supporting information). The guest molecule **G** was encapsulated by CB[7] and their assembly was investigated by ^{1}H NMR, UV-vis absorbance spectra and fluorescence spectra. Due to the poor solubility of **G** in aqueous solution, **G'** was synthesized as a reference compound. The synthetic route and corresponding characterizations of **G'** were shown in Scheme S2 and Figs. S4-S6 (Supporting information). The ^{1}H NMR spectra showed that the aromatic protons of **G'** shifted to upfields indicated the **G'** was encapsulated by the cavity of CB[7] (Fig. S7 in Supporting information). Further, the UV-vis spectra were tested and showed the absorption peak of **G** generated bathochromic shift after encapsulated by CB[7] with the purple color darkened (Fig. 1a). The Job's plot according to the ab-

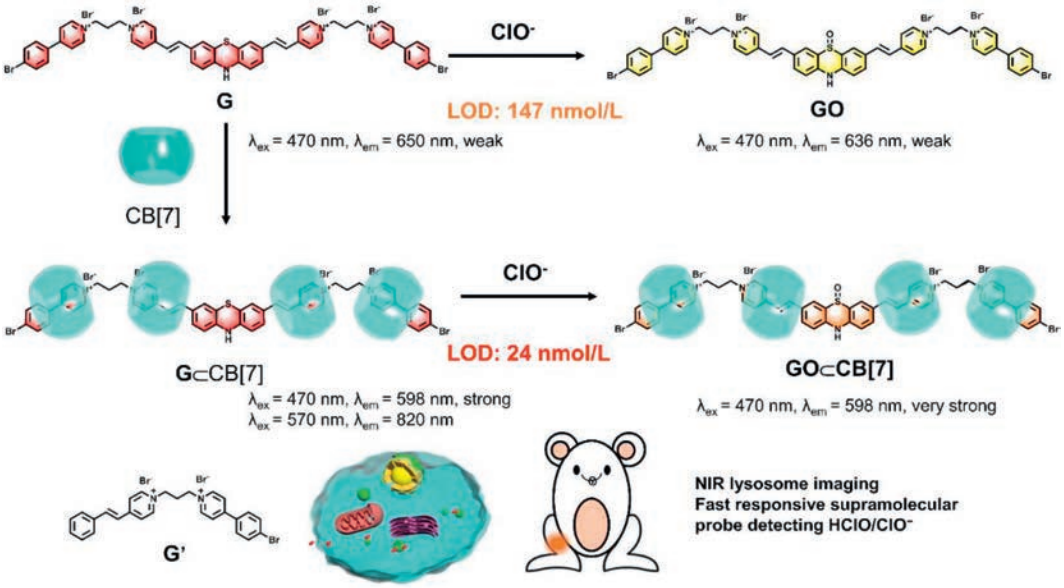

Scheme 1. Schematic diagram and applications of the supramolecular probe **G**⊂CB[7] (LOD: limit of detection).

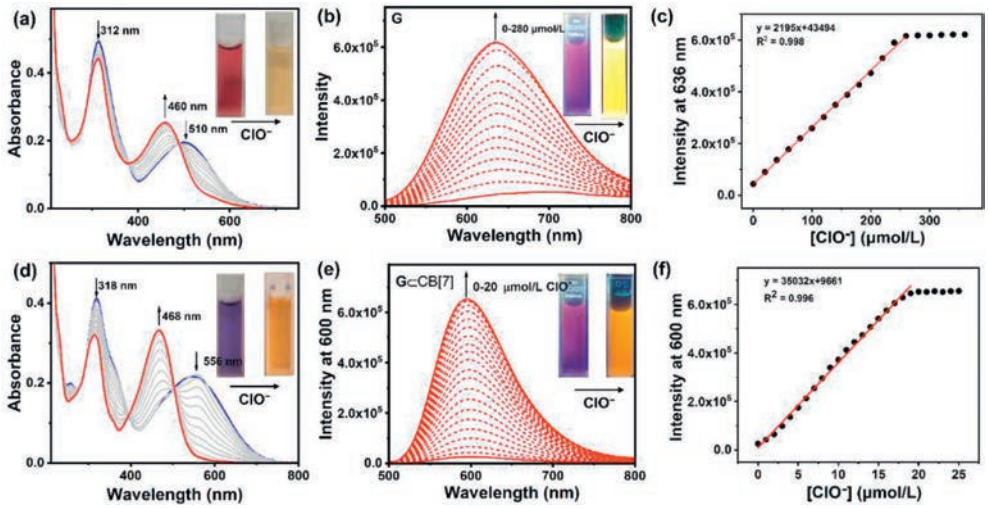

Fig. 2. (a) UV-vis absorbance spectra (inset: images of **G** under daylight). (b) Fluorescence emission spectra (inset: images of **G** under 365 nm light) and (c) fluorescence intensities of **G** (5×10^{-5} mol/L) upon addition of ClO^- (0-360 μmol/L, $\lambda_{ex} = 470$ nm, 298 K). (d) UV-vis absorbance spectra (inset: images of **G**⊂CB[7] under daylight). (e) Fluorescence emission spectra (inset: images of **G**⊂CB[7] under 365 nm light) and (f) fluorescence intensities of **G**⊂CB[7] ([**G**] = 5×10^{-5} mol/L, CB[7] = 2×10^{-4} mol/L) upon addition of ClO^- (0-25 μmol/L, $\lambda_{ex} = 470$ nm, 298 K). The above experiments were conducted in PBS (0.01 mol/L, pH 7.2-7.4).

sorption intensity of **G** and CB[7] with different concentration ratio at 318 nm showed their optimal binding ratio was 1:4 (Fig. 1b). With the gradual addition of different concentration of CB[7], the fluorescence of **G** generate hypsochromic shift to 598 nm and the intensity enhanced 103-fold (Fig. 1c). According to the intensity of **G** with different concentration of CB[7] at 598 nm, the apparent binding constant was calculated as 4.6×10^5 L/mol (Fig. 1d).

Considering the oxidizable nature of fluorophore 3,7-divinyl substituted 10*H*-phenothiazine [33], the $HClO/ClO^-$ detection ability of probes **G** and **G**⊂CB[7] was investigated by UV-vis spectra and fluorescence emission spectra. First, the absorbance spectra of **G** and **G**⊂CB[7] in aqueous solution were monitored in the air. As shown in Fig. S8 (Supporting information), **G** can be oxidized by the oxygen after exposed to air for more than 10 min. However, the supramolecular assembly **G**⊂CB[7] showed good stability in air even for 150 min. It is reasonable to believe that the encapsulation by CB[7] limited the intramolecular charge transfer which made the **G** more stable in air. Then the absorbance spectra of **G** and **G**⊂CB[7] with the gradual addition of NaClO were tested. As shown in Fig. 2a, the absorption peaks at 312 nm and 510 nm of **G** decreased and a new absorption peak at 460 nm appeared and increased with the gradual addition of NaClO, accompanying the color changed from red to yellow in phosphate buffered saline (PBS). The addition of NaClO caused the fluorescence of **G** large hypsochromic shift and intensity enhancement with the emission color changed from pink to yellow (Fig. 2b). Meanwhile, the quantum yield increased from 2.58% to 23.46% (Fig. S10 in Supporting information). According to the fluorescence intensity of **G** at 636 nm, a linear relationship between the fluorescence intensity and the concentration of NaClO was obtained (Fig. 2c) and the oxidation reaction completed upon addition of 5.2 equiv. NaClO (260 μmol/L). And the limit of detection (LOD) was calculated as 147 nmol/L according to the equation LOD = 3σ/slope. Similarly, the absorption peaks at 318 nm and 556 nm of **G**⊂CB[7] decreased and a new peak at 468 nm appeared and increased with the gradual addition of NaClO, accompanying the color changed from purple to yellow under daylight (Fig. 2d). And the fluorescence intensity of **G**⊂CB[7] increased rapidly until the concentration of NaClO reached to 20 μmol/L (Fig. 2e) with the emission color changed from pink to orange. Further, the linear relationship between the fluorescence intensity at 600 nm of supramolecular probe **G**⊂CB[7] and concentration of NaClO was obtained (Fig. 2f) and the LOD was calculated as 24 nmol/L less than the LOD of **G**, which implied the encapsulation by macrocycle enhanced the detection sensitivity of probe towards $HClO/ClO^-$. According to previous report [34] we assumed that the divalent sulphur of **G** was oxidized to sulfoxide by NaClO and its fluorescence was turned on. Subsequently, the time-depended absorbance of probes **G** and **G**⊂CB[7] to $HClO/ClO^-$ were tested. The results were shown in Fig. S9 (Supporting information) which indicated that both the oxidation progress of **G** (45 s) and **G**⊂CB[7] (13 s) finished in a few seconds. In addition, the HRMS of oxidation product of **G** by ClO^- was same to **GO** which verified that the sulfur atom of **G** was oxidized to sulfoxide as reported (Fig. S11 in Supporting information) [31].

Further, the fluorescence spectra of **G**⊂CB[7] excited by different wavelength light ranging from 400 nm to 600 nm were tested and showed that a NIR fluorescence peak appeared at 820 nm when excited by light ranging from 560 nm to 600 nm (Fig. 3a). Further, the fluorescence spectra of **G** with different concentration of CB[7] from 0 μmol/L to 250 μmol/L excited by 570 nm were tested and

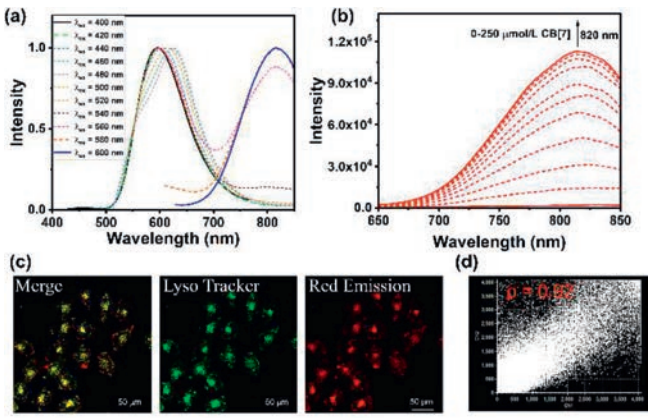

Fig. 3. (a) Normalized fluorescence spectra of **G**⊂CB[7] excited by different light ranging from 400 nm to 600 nm ([**G**] = 5×10^{-5} mol/L, [CB[7]] = 2×10^{-4} mol/L). (b) Fluorescence spectra of **G** ([**G**] = 5×10^{-5} mol/L) with the addition of CB[7] (0-250 μmol/L, $\lambda_{ex} = 570$ nm). (c) CLSM images of HeLa cells co-stained with **G**⊂CB[7] and Lyso Tracker Green. The excitation wavelengths were set as 559 nm and 405 nm, respectively ([**G**] = 2×10^{-5} mol/L, [CB[7]] = 8×10^{-5} mol/L, scale bar = 50 μm). (d) Confocal laser Pearson's correlation coefficient for lysosome co-localization images of **G**⊂CB[7]. Solvent: water.

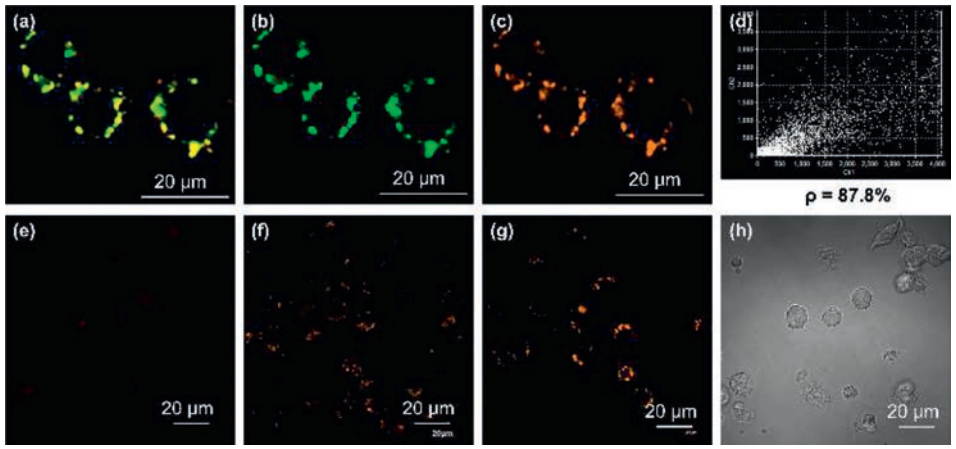

Fig. 4. CLSM images of RAW 264.7 cells co-stained with **G**⊂CB[7] and Lysotracker Green ([**G**] = 2×10^{-5} mol/L, [CB[7]] = 8×10^{-5} mol/L). (a) Merged, (b) green channel, (c) orange channel and (d) confocal laser Pearson's correlation coefficient for lysosome co-localization images of **G**⊂CB[7]. CLSM images of RAW 264.7 cells co-stained with **G**⊂CB[7]. (e) Red channel (excitation wavelength was set as 559 nm). (f) Cells were incubated with NaClO (20 μmol/L) for 20 min. (g) Cells were incubated with LPA (1 μg/mL) for 5 h and further incubated with PMA (1 μg/mL) for 20 min. (h) Bright field image. The excitation wavelengths were set as 458 nm unless otherwise indicated. Scale bar: 20 μm.

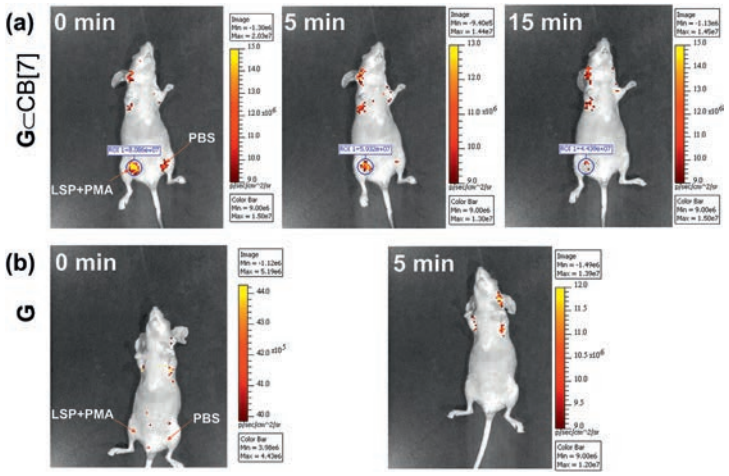

Fig. 5. *In vivo* bioimaging of nude mice after a skin-pop injection of LPS (100 μL × 1 μg/mL) for 12 h and then PMA (50 μL × 1 μg/mL) for 30 min at left and PBS at right and further injection at both parts with (a) **G**⊂CB[7] and (b) **G** for different time ([**G**] = 2×10^{-5} mol/L, [CB[7]] = 8×10^{-5} mol/L), λ_{ex} = 465 nm, optical imaging windows at DsRed, 298 K).

presented a gradually enhanced NIR fluorescence. Considering the higher penetrability in tissue and lower phototoxicity of NIR light, the supramolecular assembly **G**⊂CB[7] was applied to cell imaging. First, the biotoxicity of **G**⊂CB[7] was tested using HeLa cells as model by cell counting kit-8 (CCK-8) assay. As shown in Fig. S12a (Supporting information), the supramolecular assembly **G**⊂CB[7] showed almost no toxicity to HeLa cells with the concentration even reach to 50 μmol/L. And confocal laser scanning microscope (CLSM) was used to observe the distribution of supramolecular assembly **G**⊂CB[7] in cells. HeLa cells were incubated with **G**⊂CB[7] for 12 h and then co-incubated with Lysotracker Green for 30 min. As shown in Fig. 3c, the red emission in cells excited by 559 nm light coincide well with the green emission (Lysotracker Green) excited by 405 nm light. And the Pearson correlation coefficient reached 0.92 (Fig. 3d), which implied the lysosome-targeted ability of supramolecular assembly **G**⊂CB[7].

The excellent detection performance of **G**⊂CB[7] to HClO/ClO^- making the detection of intracellular HClO/ClO^- possible. RAW 264.7 cells were used as a model to test the detection ability of **G**⊂CB[7] to exogenous HClO/ClO^-. First, the biotoxicity of **G**⊂CB[7] to RAW 264.7 cells was tested by CCK-8 method which showed lower toxicity when the concentration lower than 30 μmol/L (Fig. S12b in Supporting information). Then, RAW 264.7 cells were incubated with **G**⊂CB[7] for 4 h and then co-incubated with Lysotracker Green for 20 min. As shown in Figs. 4a-d, the CLSM images showed that the **G**⊂CB[7] accumulated in lysosome of RAW 264.7 cells with Pearson correlation coefficient of 0.878, which was consistent with the HeLa cells. It is well known that macrophages can produce endogenous HClO when stimulated by lipopolysaccharide (LPS) and phorbol myristate acetate (PMA) [35]. Further, RAW 264.7 cells were incubated with **G**⊂CB[7] for 4 h and then used to detect endogenetic and exogenic HClO/ClO^-. As shown in Fig. 4e, there was no signal can be observed when RAW 264.7 cells were incubated with **G**⊂CB[7] only. And then further addition of NaClO (Fig. 4f) or co-incubated with LPA (1 μg/mL) for 5 h and further incubated with PMA (1 μg/mL) for 20 min (Fig. 4g), significant orange emission can be seen in RAW 264.7 cells. These results implied that **G**⊂CB[7] can detected both endogenetic and exogenic HClO/ClO^-.

Encouraged by the outstanding detection ability of **G**⊂CB[7] to HClO/ClO^- *in vitro*, the supramolecular probe was used to detect endogenous HClO/ClO^- with nude mice as model. As reported, the macrophages and neutrophils in an acute inflammation model caused by LPS can produce HClO [36]. In the experiments, solu-

tion of LPS (100 μL × 1 μg/mL) and PMA (50 μL × 1 μg/mL) were injected into the right hindlimbs of two nude mice and then **G**⊂CB[7] or **G** was injected into the same place, respectively. As control, PBS was injected to the left hindlimbs of the two nude mice and then **G**⊂CB[7] or **G** was injected into the same place, respectively. As shown in Fig. 5a, obvious fluorescence was observed at the right hindlimbs of mouse immediately and lasted for 15 min. While there was almost no signal can be observed both at the left hindlimbs of the same mouse and the other mouse treated with probe **G** (Fig. 5b). The above experiments verified that supramolecular probe **G**⊂CB[7] showed good detection ability to HClO/ClO^- *in vivo*.

In summary, we conjugated electron-withdrawing group 4-(4-bromophenyl)pyridine to fluorophore 3,7-divinyl substituted 10*H*-phenothiazine and obtained a water-soluble compound (**G**) whose LOD toward HClO/ClO^- was calculated to be 147 nmol/L. After encapsulated by CB[7], the fluorescence intensity and stability in air of **G** increased significantly and showed a NIR fluorescence at 820 nm when excited by 570 nm light. And the LOD towards HClO/ClO^- of the supramolecular probe was calculated to be 24 nmol/L. Subsequently, the supramolecular probe (**G**⊂CB[7]) was applied to NIR lysosome imaging and detection of both exogenous and endogenous HClO/ClO^- in RAW 264.7 cells and nude mice. All in all, a macrocycle encapsulation enhanced fluorescent probe for detection of HClO/ClO^- with NIR emission was constructed through the macrocycle confinement effect caused by host-guest assembly, which provide an easy way to constructed biomarkers.

Declaration of competing interest

The authors declare that they have no known competing financial interests or personal relationships that could have appeared to influence the work reported in this paper.

Acknowledgments

This work was financially supported by the National Natural Science Foundation of China (No. 22131008) and Liaocheng University Start-up Fund for Doctoral Scientific Research (No. 318052327). The experiments were also assessed by the Animal Experimentation Ethics Committee of Nankai University, and the assigned approval number is 2021-SYDELL-000448.

Supplementary materials

Supplementary material associated with this article can be found, in the online version, at doi:10.1016/j.cclet.2023.109183.

References

[1] X.K. Ma, Y. Liu, Acc. Chem. Res. 54 (2021) 3403–3414.
[2] T. Zhang, X. Ma, H. Wu, et al., Angew. Chem. Int. Ed. 59 (2020) 11206–11216.
[3] Z. Liu, Y. Liu, Chem. Soc. Rev. 51 (2022) 4786–4827.
[4] H.J. Wang, M.M. Zheng, W.W. Xing, et al., Chem. Sci. 14 (2023) 8401–8407.
[5] H.J. Wang, H.Y. Zhang, W.W. Xing, et al., Chin. Chem. Lett. 33 (2022) 4033–4036.
[6] G. Qu, Y. Zhang, X. Ma, Chin. Chem. Lett. 30 (2019) 1809–1814.
[7] H. Nie, Z. Wei, X.L. Ni, Y. Liu, Chem. Rev. 122 (2022) 9032–9077.
[8] H.J. Wang, W.W. Xing, H.Y. Zhang, W.W. Xu, Y. Liu, Adv. Optical Mater. 10 (2022) 2201178.
[9] W.W. Xing, H.J. Wang, Z. Liu, et al., Adv. Optical Mater. 11 (2023) 2202588.
[10] D.A. Xu, Q.Y. Zhou, X. Dai, et al., Chin. Chem. Lett. 33 (2022) 851–854.
[11] H.J. Wang, W.W. Xing, Z.H. Yu, et al., Adv. Optical Mater. 10 (2022) 2201903.
[12] C. Li, X. Li, Q. Wang, Chin. Chem. Lett. 33 (2022) 877–880.
[13] W.L. Zhou, Y. Chen, Q. Yu, et al., Nat. Commun. 11 (2020) 4655.
[14] H.J. Yu, Q. Zhou, X. Dai, et al., J. Am. Chem. Soc. 143 (2021) 13887–13894.
[15] Z.Y. Zhang, Y. Chen, Y. Liu, Angew. Chem. Int. Ed. 58 (2019) 6028–6032.
[16] Z.Y. Zhang, Y. Liu, Chem. Sci. 10 (2019) 7773–7778.
[17] X.K. Ma, Q. Cheng, X. Zhou, Y. Liu, JACS Au 3 (2023) 2036–2043.
[18] J. Song, L. Ma, S. Sun, H. Tian, X. Ma, Angew. Chem. Int. Ed. 61 (2022) e202206157.
[19] D. Li, Z. Liu, M. Fang, et al., ACS Nano 17 (2023) 12895–12902.
[20] X. Chen, X. Tian, I. Shin, J. Yoon, Chem. Soc. Rev. 40 (2011) 4783–4804.
[21] D. Shi, S. Chen, B. Dong, et al., Chem. Sci. 10 (2019) 3715–3722.
[22] L. Behrend, G. Henderson, R.M. Zwacka, Biochem. Soc. Trans. 31 (2003) 1441–1444.
[23] S.V. Mulay, M. Choi, Y.J. Jang, et al., Chem. Eur. J. 22 (2016) 9642–9648.
[24] S.I. Grivennikov, F.R. Greten, M. Karin, Cell 140 (2010) 883–899.
[25] Y. Hirabayashi, Mod. Rheumatol. 31 (2021) 966–971.
[26] H. Feng, Z. Zhang, Q. Meng, et al., Adv. Sci. 5 (2018) 1800397.
[27] H. Zhu, J. Fan, J. Wang, H. Mu, X. Peng, J. Am. Chem. Soc. 136 (2014) 12820–12823.
[28] Z. Mao, M. Ye, W. Hu, et al., Chem. Sci. 9 (2018) 6035–6040.
[29] X.B. Wang, H.J. Li, Q. Li, et al., J. Hazard. Mater. 427 (2022) 127874.
[30] H.H. lin, C.C. chang, Dyes Pigments 83 (2009) 230–236.
[31] P. Wu, H. Xiong, Talanta 247 (2022) 123584.
[32] R. Shi, H. Chen, Y. Qi, et al., Analyst 144 (2019) 1696–1703.
[33] Y. Zhang, P. Gao, X. Guo, et al., RSC Adv. 10 (2020) 16732–16736.
[34] Y. Rout, A. Ekbote, R. Misra, J. Mater. Chem. C 9 (2021) 7508–7531.
[35] Y. Adachi, A.L. Kindzelskii, A.R. Petty, et al., J. Immunol. 176 (2006) 5033–5040.
[36] K. Kundu, SF. Knight, N. Willett, et al., Angew. Chem. Int. Ed. 48 (2009) 299–303.